Development of Counter-facing Discharge Device for Extreme Ultraviolet Source
~ Evaluation of Electrode Damages for Stationary Operation ~

Daisuke Nishii, Kouki Kanou*, Tomoaki Kawasaki*, Tatsuya Sodekoda**, Hajime Kuwabara**, Mitsuo Nakajima*, Kazuhiko Horioka*

Department of Mechano-Aerospace Engineering, Tokyo Institute of Technology
2-12-1 Ookayama, Meguro-ku, Tokyo, 152-8550, Japan

**Department of Energy Sciences, Tokyo Institute of Technology*
4259 Nagatsuta-cho, Midori-ku, Yokohama, Kanagawa, 226-8503, Japan

***Advanced Applied Department, IHI Corporation*
1 Shin-nakahara-cho, Isogo-ku, Yokohama, Kanagawa, 235-8501, Japan

ABSTRACT

Center electrode damages of couter-facing discharge device for Extreme Ultraviolet(EUV) source were classified to stationary damage and pulsed damage. We estimated stationary thermal load by using a semi-empirical simulation. As a results, we found that the electrode temperature becomes too hot under the stationary operation. Also, we examined pulsed thermal load by establishing a simplified model based on the Child-Langmuir sheath. The results showed that the calculation over-estimated the sheath potential, which showed the need to develop a self-consistent model which can deal with the plasma sheath boundary.

Keywords

Key Words: EUV Light Source, Plasma Focus, Thermal Damage, Sheaths, High energy density plasma

1 Introduction

Integrated circuits(ICs) are indispensable for our moden society. Performance of ICs basically depends on the scale of the integration, so raising of the accumulation rate is the first priority. ICs are usually processed by photolithography, and the minimum working size depends on wavelength of the light source [1]. Therefore, development of a shorter wavelength light source is important. What expected for the next generation lithography is Extreme Ultraviolet(EUV) light source, which means 13.5 nm wavelength light here, and it is contained in a radiation from a high energy density plasma.

For industrial use, the way of making the high energy density plasma is classified into Laser Produced Plasma(LPP) or Discharge Produced Plasma(DPP). In LPP scheme, a high energy density plasma is produced by irradiating a high intensity laser to the target. LPP is easy to be controled, but the energy conversion efficiency is basically very low. In DPP scheme, a high energy density plasma is produced by a pulsed discharge. DPP has high energy conversion efficiency, but the electrode damage is a serious issue to be solved and is difficult to manage due to the complex nature of the discharge process.

To develop an efficient EUV light source, we have developed a plasma device which has counter-facing plasma focus electrodes. By the research and development of this device so far, we have attained a 100 mJ EUV output per 1 operation [2]. For the next step, we are aiming at repetitive operation at 1 kHz, but there are some problems. One of them is the thermal damage of the electrode because of the load of high current and the electron spattering. Electrode thermal damages can be classified to two types. The first is a stationary damage due to the Joule heating and heat-flow through

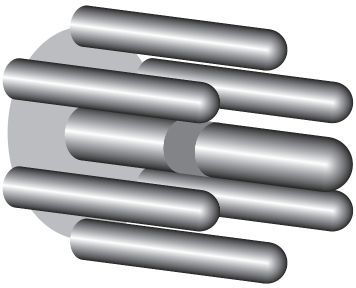

Fig. 1. Configration of one side electrodes in couter-facing discharge plasma focus device.

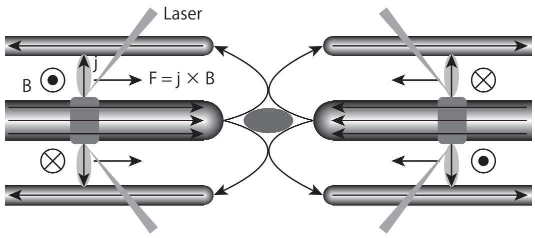

Fig. 2. Schematic of operation of counter-facing plasma focus system.

the sheaths, the second is a pulsed damage due to arc-discharge. To achieve repetitive operation for long periods, these damages should be suppressed under a permissible limit.

The purpose of this research is to evaluate the electrode thermal damages quantitatively and examine the condition in which electrode thermal damages are kept under the permissible limit.

2 Experimental Setup and Method of Evaluation of Electrode Thermal Damages

2.1 Counter-facing Discharge Plasma Focus Device

We have developed a counter-facing discharge device which is composed of a pair of six-channel plasma focus electrodes. Figure 1 shows the focus device composed of a center electrode and six outer electrodes. The plasma source(lithium) is embedded in a groove of the center electrode. Figure 2 schematically shows the operation of the device to make EUV plasma. At first, capacitors between a center electrode and independent six outer electrodes are charged to high voltage(5~7kV). A laser irradiates the plasma source at middle of the center electrodes and makes the plasma. Then, currents start to flow between the center electrode and the outer electrodes through plasma. The plasma is accelerated to the center of the counter-facing electrodes by the Lorentz force. The counter-facing plasma driven by the current sheets collide and thermalize at the center, where it is confined by the Lorentz force. Then, a high energy density EUV plasma is generated.

2.2 Numerical Analysis of Stationary Thermal Load

In the plasma focus device, the current flows with a time constant of μsec and the heat deposition in the electrode diffuses with order of msec. Therefore, the electrode temperature repeats rise and down. But in a time scale longer than the time constant, the electrode temperature can be regarded as having a simply rising character. We call such a heat inflow as a ”stationary load” here.

Stationary thermal load raises the electrode temperature, and the temperature distribution can be obtained by solving a thermal diffusion equation. In two-dimensional cylindrical coordinates system, the thermal diffusion equation is given as follows,

$$\frac{\partial T}{\partial t} = a\left(\frac{\partial^2 T}{\partial r^2} + \frac{1}{r}\frac{\partial T}{\partial r} + \frac{\partial^2 T}{\partial z^2}\right) + q(r,z) \ , \qquad (1)$$

where T is the electrode temperature at (r, z), a is thermal diffusivity, $q(r,z)$ is internal heating term [3]. We made a numerical simulation code with two-dimensional cylindrical coordinate system and evaluated the electrode temperature.

2.3 Sheath Modeling for Evaluating Pulsed Thermal Load

When the discharge current is localized at a point of electrode surface, an arc discharge may occur. The arc discharge damages the electrode. We call this damage as a ”pulsed thermal load” here.

To evaluate the pulsed thermal load, it is important to understand the sheath dynamics. But there is no es-

Tab. 1. Parameters for thermal calculation.

Parameter	Value
Material of electorode	W(head), Cu(root)
Length of electrode	32.5 mm
Curvature of electrode head	1.5 mm
Charging voltage of capacitor	7 kV
Pulse rate	1 kHz
Sheath heat	270 W
Cooling temperature	200 ℃

Tab. 2. Physical properties of electrode materials.

Parameter	Tungsten	Copper
Melting temperature [K]	3700	1450
Thermal conductivity [W/mK]	173	401
Specific heat [J/gK]	0.138	0.379
Mass density [g/cm^3]	0.138	0.379
Electrical resistivity [nΩm]	52.8	16.8

Tab. 3. Conditions for numerical calculation.

Parameter	Value
Time step Δt	1.0×10^{-5} sec
Division number of z-axis	300
Division number of r-azis	30

tablished model about the sheath dynamics. So we are developing a new sheath dynamics model.

3 Results and Discussion

3.1 Numerical Simulation for Evaluating Stationary Thermal Load

3.1.1 Analysis conditions

Table 1 shows basic parameters of the numerical study. Table 2 shows physical properties of the electrode materials, and Tab. 3 represents the conditions for the numerical calculation.

3.1.2 Time to achieve quasi-steady state

Figure 3 shows temporal evolution of the electrode head temperature. As the figure shows, it takes about 10 sec to achieve the quasi-steady temperature distribution. In other words, we can reach a steady state temperature distribution by the time integration of Eq. (1) for 10 sec.

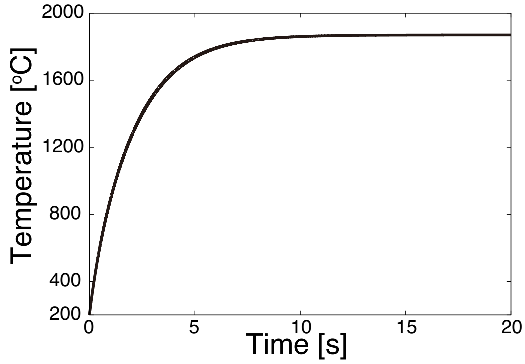

Fig. 3. Evolution of electrode head temperature.

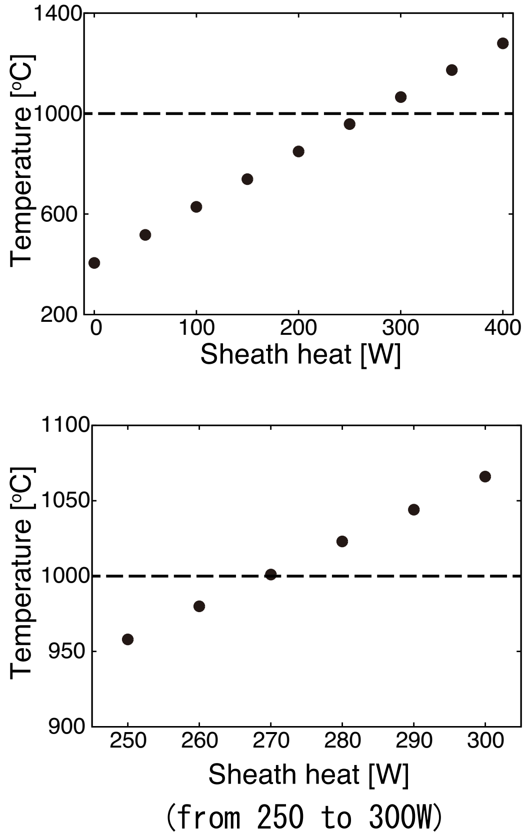

Fig. 4. Temperature change of electrode head as a function of sheath heating power.

3.1.3 Evaluation of sheath heating by parameter survey

It is difficult to evaluate the sheath heating phenomenom with a numerical modeling. So we tried to evaluate the sheath heating semi-empirically, namely by fitting the numerical calculation with the experimental observation. We know that temperature of the elec-

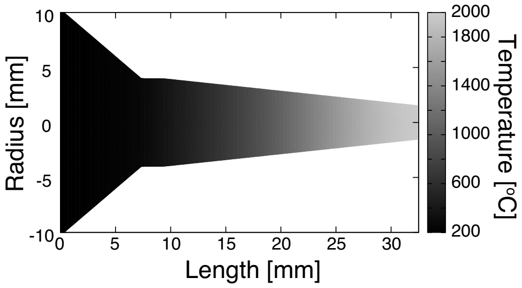

Fig. 5. Typical electrode temperature distribution.

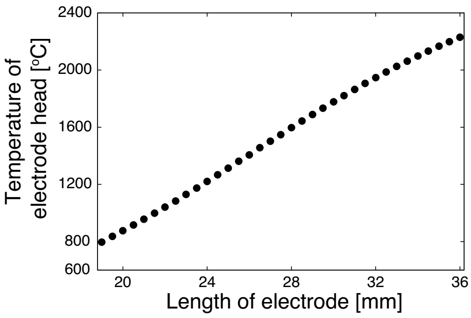

Fig. 6. Temperature change of electrode versus electrode length.

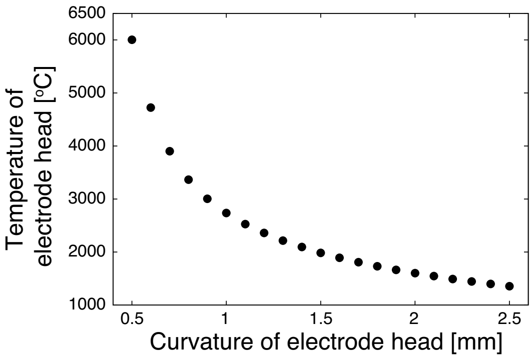

Fig. 7. Temperature change of electrode as a function of electrode head curvature.

trode head reaches around 1000 ℃ when the plasma focus device operated for 1 second at 1 kHz. Figure 4 shows the temperature change of electrode head as a function of sheath heating power ranging from 0 W to 400 W. As Fig. 4 shows, the sheath heating corresponding to the electrode temperature is estimated to be 270 W. After this, we regard the sheath heating as 270 W.

3.1.4 Change of the electrode temperature when the electrode shape is changed

EUV output depends on the electrode configuration [4], and it is expected that the electrode temperature also depends on the electrode shape. So we varied the electrode length form 19.0 mm to 36.0 mm and the electrode head curvature from 0.5 mm to 1.5 mm. Figure 5 shows a typical electrode temperature distribution in the case of condition shown in Tab. 1 . As it shows, we know that the electrode head temperature rises about 2000 ℃.

Figure 6 shows the temperature change of the electrode when the electrode length is changed and Fig. 7 shows the temperature as a function of the electrode head curvature. As these results show, the electrode temperatures decrease as the electrode becomes shorter or the electrode head curvature becomes bigger. The results also show that if we suppose that the temperature limit of tungsten is 1000 ℃, the electrode length has to be shorter than 22 mm or the electrode head curvature has to be bigger than 2.5 mm. But from the point of view of EUV output, this geometry is not optimum, so we have to consider a rational cooling system to optimize the electrode geometry for EUV conversion.

3.1.5 Change of the thermal temperature distribution when the input power is changed

If we increase the input power, EUV output is expected to be increased, but the electrode temperature is also expected to increase. It is important to examine the input power limit, so we made analysis when input power is changed. Experimental results show that when the charge voltage of capacitor is raised, EUV output increases. So we varied the voltage of capacitors from 5 KV to 7 kV. Also, we varied the repetition frequency from 1 kHz to 10 kHz. Figure 8 shows the temperature change of the electrode head versus the charging voltage and Fig. 9 shows the temperature versus repetition frequency. As shown, the electrode head temperature increases as the input power is raised. We are aiming

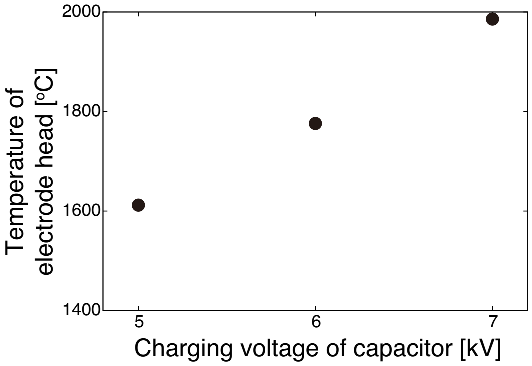

Fig. 8. Temperature change of electrode head versus charging voltage.

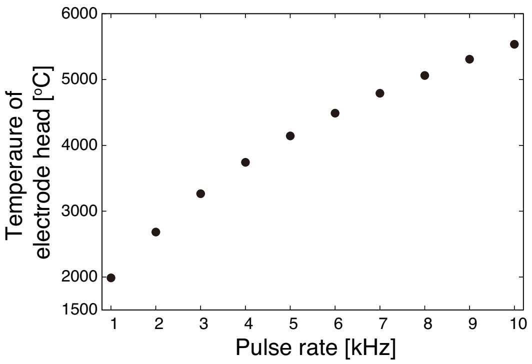

Fig. 9. Temperature change of electrode head versus repetition frequency.

at a continuous operation at 10 kHz, but the head load limits the repetition less than 3 kHz to avoid the melting of tungsten electrode. So we have to improve the energy conversion efficiency.

3.2 Modeling the Sheath Physics for Evaluating Pulsed Heat-inflow

3.2.1 Evaluating the Sheath Potential from the Child-Langmuir Law

Generation of arc spots depend on the sheath potential and width. They can be evaluated from the Child-Langmuir law. The Child-Langmuir law is given by

$$j = \frac{4}{9}\varepsilon_0 \left(\frac{2e}{m_\mathrm{i}}\right)^{1/2} \frac{\phi^{3/2}}{d^2}\ , \tag{2}$$

where j is the current density, ε_0 is the permittivity of free space, e is the elementary charge, m_i is the mass of ion, ϕ is the sheath potential, d is the sheath width [5]. We can know j because j is primarily determined by the external circuit in case of the discharge plasma device. So ϕ can be calculated using Eq. (2) by assuming d. Generally, the sheath width d is considered to be the order of the Debye length λ_d given by

$$\lambda_d = \left(\frac{\varepsilon_0 k_\mathrm{B} T_\mathrm{e}}{n_\mathrm{e} e^2}\right)^{1/2}\ , \tag{3}$$

where k_B is the Boltzmann constant, T_e is the electron temperature, n_e is the electron density. The sheath potential ϕ is calculated as shown in Fig. 10 . In the calculation, we assumed $d = 10\lambda_d$, $T_\mathrm{e} = 10\,\mathrm{eV}$, $n_\mathrm{e} = 1.0 \times 10^{14}\,\mathrm{cm}^{-3}$ and $m_\mathrm{i} = 1.15 \times 10^{-26}\,\mathrm{kg}$(lithium). As shown, the sheath potential was obviously much larger than real one. So we have to develop a self-consistent model which can deal with plasma and sheath dynamics.

4 Conclusions

We estimated stationary temperature distribution of the center electrode by numerical simulations and compared it with experimental observation. We found that time to achieve the quasi-steady state is 10 sec and the sheath heating is ~ 270 W. The results also indicate that the electrode head temperature reaches around 2000 ℃ in typical conditions at a steady operation. If we assume that the electrode limit temperature is 1000 ℃, we have to improve the cooling system and/or increase the energy conversion efficiency.

Also we calculated the sheath potential using the Child-Langmuir law for evaluating the pulsed thermal

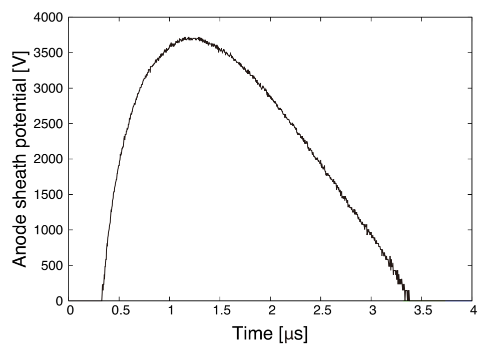

Fig. 10. Calculated sheath potential assuming the Child-Langmuir sheath.

load. The calculation over-estimated the sheath potential, so we have to consider a model which can deal with the plasma and the sheath without contradiction.

References

[1] S. KOBAYASHI, T. KOTANI, and S. KYOH. "Design for Manufactureability Technology to Accelerate Advanced Semiconductor Lithograohy Processes". *TOSHIBA review*, **66**(5):25–28, (2011).

[2] T. Sodekoda, H. Kuwabara, M. Masashi, S. Liu, K. Kanou, K. Kawaguchi, and K. Horioka. "Repetotove operation of counter-facing plasma focus device: toward a practical light source for euv lithography". **9048**:904824–904824–8, (2014).

[3] R. Bird, W. Stewart, and E. Lightfoot. *Transport Phenomena*. Wiley International edition. Wiley, (2007).

[4] K. Kanou, T. Kawasaki, D. Nishii, H. Kuwabara, T. Sodekoda, A. Tokuchi, and K. Horioka. "Quasi-steady operation of counter-facing plasma-focus device for high-average-power radiation source in extreme ultraviolet region". *PROCEEDINGS OF PLASMA CONFERENCE 2014*, (2014).

[5] A. T. Forrester. *Large Ion Beams Fundamentals of Generation and Propagation*. Wiley, (1988).